Available online at www.sciencedirect.com
ScienceDirect
Ocean Engineering 34 (2007) 479–488
OCEAN ENGINEERING
www.elsevier.com/locate/oceaneng

On the track keeping and roll reduction of the ship in random waves using different sliding mode controllers

Ming-Chung Fang*, Jhih-Hong Luo

Department of Systems and Naval Mechatronic Engineering, National Cheng Kung University, Tainan 701, Taiwan, ROC

Received 4 November 2005; accepted 1 March 2006
Available online 19 June 2006

Abstract

In the paper, an autopilot system composed of sliding mode controller and line-of-sight guidance technique are adopted to navigate the ship in random waves by altering the rudder deflection. Two kinds of sliding mode controller are considered; one is the separate system including sway–yaw control and roll control, the other is the compact system considering sway–roll–yaw control altogether. Both track keeping and roll reduction are accomplished by rudder control and the design parameters of controller are optimized by genetic algorithm. The present simulation results show both the separate controller and the compact controller work quite well, either for track keeping or roll reduction while the ship is sailing in random waves. However, the separate controller is recommended due to its simplicity.

Keywords: Track keeping; Roll reduction; Sliding mode control; Genetic algorithm

1. Introduction

With the development of automation technology, many ships use the autopilot system to reduce helmsman's workload. The use of the autopilot within the navigation systems has successfully overcome the problem of the course keeping of ships. The PD controller (Munif and Umeda, 2000; Umeda and Hashimoto, 2002) and PID controller (Dove and Wright, 1991) with fixed design parameters are conventional autopilot systems for ship steering, which are the most widely used among many autopilot systems because of its simplicity. McGookin et al. (2000) adopted the sliding mode control law for rudder control to simulate the course changing control and track keeping control of a tanker. They also used genetic algorithms to optimize the design parameters, but the wave effect was not investigated.

Since the ship is always sailing in the seaway, the wave disturbances will affect the ship motions, especially on the roll motion. Large roll motion may cause cargo damage and reduce the effectiveness of crews because of seasickness and tiredness. For some ships, landing a helicopter will become more difficult when the roll motion is too large. The worst situation is if the ship is unable to counteract the large roll motion, the operation may be suspended and may lead the capsizing. In a word, the serious roll motion generally affects the ship stability, comfort and efficiency of screws, accuracy of electrical mechanism, and ship course. Therefore reducing roll motion is advantageous for ships in waves.

Some devices have been well employed to accomplish roll reduction, e.g. bilge keels, anti-roll tanks, gyroscopic stabilizers, moving weights, and stabilizing fins (Treakle et al., 2000). Although most of the devices work well, additional devices and external power installations will lead to the weight increase and space decrease on the ship. The hydrodynamic stability and structural strength may be changed when the anti-roll tanks are adopted. The installation cost is also generally raised and the ship speed may be decreased because of additional appendages. Usually most ships use rudder to alter the course and it is known that the rudder action will cause some roll motion even in calm water. It means the rudder can produce an additional roll moment and therefore can then be regarded

*Corresponding author. Tel.: +886 6 2747018x211; fax: +886 6 2080592.
E-mail address: fangmc@mail.ncku.edu.tw (M.-C. Fang).

0029-8018/$ - see front matter © 2006 Elsevier Ltd. All rights reserved.
doi:10.1016/j.oceaneng.2006.03.004

as a roll reduction device if the ship's course is not violently altered. The roll reduction using the rudder control technique has been proposed for two ships doing underway replenishment (Fang, 1991) and for a single ship sailing in waves (Jerrold and Michael, 1999). The US navy also completed a series of rudder roll stabilization investigations on a destroyer and found the reduction in roll motion is about 40% (Baitis and Schmidt, 1989). The results indicate that it is possible to reduce roll motion by using rudder control, and this effect can be more significant for small high-speed vessels (Fossen, 1994).

In order to simulate the ship motion in the seaway, the mathematical model must include maneuvering and seakeeping. Some valuable information about the ship maneuvering predicted by the mathematical model in calm water for naval architects have been offered, e.g. Hirano (1980) and Inoue et al. (1981). But the mathematical model with wave effect is rather difficult to be handled because of the complexity of the hydrodynamic coupling effect between the maneuvering and seakeeping. However, several authors have developed some simplified mathematical models combining seakeeping and maneuvering for predicting the maneuvering of a ship in waves. Hamamoto and Kim (1993) and Hamamoto et al. (1994) simulated the turning circle and Zig-Zag trial of a ship sailing in waves with a six degrees of freedom model combining maneuvering and seakeeping characteristics. Bailey (1999) proposed a unified mathematical model including maneuvering and seakeeping to simulate the ship steering behavior in waves, and the relationships between maneuvering derivatives and seakeeping coefficients with encounter frequency variations are considered. Umeda and Hashimoto (2002) utilized a numerical model of surge–sway–yaw–roll motion with dense grids of control parameters and the sudden-change concept to intensively explore nonlinear ship motions in following and quartering seas and successfully explain the capsizing phenomena qualitatively. In their study, the heave and pitch motions were simply approximated from stable equilibrium because of the small encounter frequency. Funaji et al. (2003) also adopted a four degrees of freedom numerical model to simulate the turning motion and Zig-Zag maneuver with external disturbances (i.e. wave and wind).

In this study, two different sliding mode control laws, i.e. "Separate Control" and "Compact Control", are adopted to control the rudder deflection. The autopilot ability and roll reduction effect for the ship sailing in waves are investigated. The design parameters in the sliding mode controllers are tuned by genetic algorithm and the design criterion is base on the cost function composing the heading error, rudder deflection and roll motion.

2. Mathematical model

Three coordinate systems are used to describe the present mathematical model (Hamamoto et al., 1994). The inertial coordinate system $O-X_0Y_0Z_0$ is fixed on the calm water surface and used to describe the wave. The body coordinate system $G-xyz$ with its origin at the ship's center of gravity is moving with the ship motion. The horizontal body coordinate system $G-x'y'z'$ is also fixed at the ship's center of gravity but $Gx'y'$ plane is always parallel to OX_0Y_0 plane. In these coordinate systems, the positive Z_0, z and z' axes are downward.

The equations of motions (1)–(6) and the corresponding forces are described by the horizontal body coordinate system. Combining simultaneously with the engine torque equation (7), we can solve the corresponding ship motions in waves:

$$\text{Surge}: \quad m(\dot{u}-v\dot{\psi}) = X_{\mathrm{HF}}+X_{\mathrm{FK}}+X_{\mathrm{DF}}+X_{\mathrm{RF}} + T(1-t_p)-R, \tag{1}$$

$$\text{Sway}: \quad m(\dot{v}+u\dot{\psi}) = Y_{\mathrm{HF}}+Y_{\mathrm{FK}}+Y_{\mathrm{DF}}+Y_{\mathrm{RF}}, \tag{2}$$

$$\text{Heave}: \quad m\dot{w} = Z_{\mathrm{HF}}+Z_{\mathrm{FK}}+Z_{\mathrm{DF}}, \tag{3}$$

$$\text{Roll}: \quad I_{xx}\ddot{\phi}-I_{xx}\dot{\theta}\dot{\psi} = K_{\mathrm{HF}}+K_{\mathrm{FK}}+K_{\mathrm{DF}}+K_{\mathrm{RF}}, \tag{4}$$

$$\text{Pitch}: \quad I_{yy}\ddot{\theta}+I_{xx}\dot{\psi}\dot{\phi} = M_{\mathrm{HF}}+M_{\mathrm{FK}}+M_{\mathrm{DF}}, \tag{5}$$

$$\text{Yaw}: \quad I_{zz}\ddot{\psi}-I_{xx}\dot{\theta}\dot{\phi} = N_{\mathrm{HF}}+N_{\mathrm{FK}}+N_{\mathrm{DF}}+N_{\mathrm{RF}}, \tag{6}$$

$$\text{Engine}: \quad 2\pi I_{\mathrm{PP}}\dot{n} = Q_{\mathrm{E}}+Q_{\mathrm{P}}. \tag{7}$$

In the above equations, m and I are ship mass and mass moment of inertia, respectively. X, Y and Z are external forces with respect to surge, sway and heave whereas K, M and N are external moment with respect to roll, pitch and yaw. Surge, sway and heave velocities are represented by u, v and w, respectively, whereas roll, pitch and yaw displacements are represented by ϕ, θ, and ψ, respectively. T is propeller thrust, R is ship resistance, and t_p is the thrust deduction coefficient. The terms I_{PP}, Q_{E}, Q_{P}, n in Eq. (7) represent the moment of inertia of propeller-shafting system, the main engine torque, the propeller torque, and the rpm of propeller, respectively. The purpose of Eq. (7) is to prevent the propeller torque over the maximum engine torque by adjusting the propeller rpm. Since the propeller thrust and torque are computed according to the propeller characteristic curve that is related to propeller rpm and ship speed, correction of the propeller rpm calculated from Eq. (7) will affect the propeller thrust, torque and six degrees of freedom motions. Subscripts HF, FK, DF, RF represent hull forces, Froude–Krylov forces, diffraction forces, and rudder forces, respectively.

The hull forces are caused by ship motion and can be described by added mass, damping and maneuvering coefficients. In order to simulate the ship motion accurately, the nonlinear maneuvering coefficients are included here. The Froude–Krylov forces are calculated by integrating the incident wave pressure acted on ship hull to the wave surface and the diffraction forces are calculated with the linear strip theory and source distribution method. Since the strip theory is applied, the wave diffraction for

surge cannot be calculated. However, it is generally small because of the slenderness of the ship and can be neglected. These forces depend on the ship configuration below the instantaneous wave surface that must be calculated at any instant time (Fang et al., 1993).

In order to simulate the random wave, the following ITTC short crest wave spectrum is adopted for simulation

$$S(\omega_i,\mu_j)=\frac{172.75H_{1/3}^2}{\bar{T}^4\omega_i^5}\exp\left(\frac{-691}{\bar{T}^4\omega_i^4}\right)\times\frac{2}{\pi}\cos^2\mu_j, \tag{8}$$

where $H_{1/3}$ is the significant wave height, $\bar{T}$ is the average period, ω_i is the wave frequency of the ith regular wave component, μ_j is the angle between main wave direction and the jth minor wave direction and $-\pi/2<\mu_j<\pi/2$. In the paper, 100 regular wave components are used to form the 2D irregular wave, then the 2D irregular waves in 11 directions (each interval between the adjacent wave directions is 15°) form the short-crested wave. Therefore, the amplitude of each regular wave component ξ_{ij} and the resultant wave ζ_w can be obtained in the following equations:

$$\zeta_{ij}=\sqrt{2S(\omega_i,\mu_j)\delta\omega\delta\mu}, \tag{9}$$

$$\zeta_w=\sum_{j=1}^{11}\sum_{i=1}^{100}\zeta_{ij}\cos\left[k_i(X_0\cos\mu_j+Y_0\sin\mu_j)-\omega_i t+\varepsilon_{ij}\right], \tag{10}$$

where k_i is the ith wave number and ε_{ij} is the random phase angle of the ith regular wave in the jth direction varied from 0 to 2π.

The resultant wave ζ_w is used to calculate the corresponding Froude-Krylov force and diffraction force. In reality, the following encounter frequency ω_e in Eq. (11) is used to calculate added masses and damping coefficients for a ship moving in irregular waves (Crossland and Johnson, 1998), which is estimated from the average frequency $\bar{\omega}$ of the spectrum, the relation is

$$\omega_e=\bar{\omega}+\bar{\omega}^2U/g\cos\psi, \tag{11}$$

where

$$\bar{\omega}=0.5\left(\frac{2\pi}{1.296\bar{T}}+\sqrt{\frac{2\pi g}{1.25L}}\right), \tag{12}$$

where U is the ship velocity and L is the ship length between perpendiculars.

In the present study, the rudder is the only device used to control the track keeping and roll reduction. The forces and moments induced by the rudder action are expressed in the following (Hirano, 1980):

$$X_{RF}=-F_N\sin\delta, \tag{13}$$

$$Y_{RF}=-(1+a_H)F_N\cos\delta, \tag{14}$$

$$K_{RF}=-z_R Y_{RF}, \tag{15}$$

$$N_{RF}=x_R Y_{RF}, \tag{16}$$

where δ is the rudder angle, F_N is the normal force on the rudder, a_H is the ratio of hydrodynamic force induced on ship hull by rudder action to rudder force, x_R and z_R are the x- and z-coordinate of the point which the rudder force Y_{RF} acts, respectively.

3. Control systems for ship track keeping and roll reduction

In this section, the autopilot controller is incorporated into Eqs. (1)–(7) to simulate the ship maneuvering with assumed waypoints. In this study, two kinds of sliding mode control systems are adopted to investigate the ship control ability. One is build by two control subsystems separately, i.e. sway–yaw and roll, that is called "Separate Control", and the other one is obtained including the whole sway–roll–yaw interactions, that is called "Compact Control".

In order to guide the ship sailing to commanded waypoints, a simple line-of-sight (LOS) guidance technique (McGookin et al., 2000) is introduced. The ship's heading angle directing to the desired waypoint position is calculated by the following formula and the illustration is shown in Fig. 1:

$$\psi_d=\tan^{-1}\left(\frac{Y_{WP}-Y_G}{X_{WP}-X_G}\right). \tag{17}$$

In the equation, $(X_G,\ Y_G)$ is the coordinate of the instantaneous ship position whereas $(X_{WP},\ Y_{WP})$ is the coordinate of the desired waypoint position. If the distance between ship position and waypoint is less than acceptable radius, next waypoint will be acquired for navigation. In this study, the acceptable radius is set as twice ship length, and the ship heading angle in Eq. (17) varies with $(X_G,\ Y_G)$ and $(X_{WP},\ Y_{WP})$.

3.1. Separate control

The separate control applies two separate sliding mode controllers to execute the track keeping and roll reduction by altering the rudder deflection. One is integrated with the LOS guidance system for track keeping and the other is applied for roll reduction. Therefore, the resultant rudder angle δ required for the ship track keeping and roll reduction can be expressed as

$$\delta=\delta_\psi+\delta_\phi, \tag{18}$$

where δ_ψ and δ_ϕ are applied for track keeping and roll reduction, respectively.

The sliding mode controller is adopted here because of its good performance robustness. This control theory has a switching action, which provides a robustness to match uncertainties. Since the rudder angle is the only input controlled in the present study, a single-input-multiple-states model (Healey and Lienard, 1993; Fossen, 1994) for track keeping control is linearized from Eqs. (2) and (6)

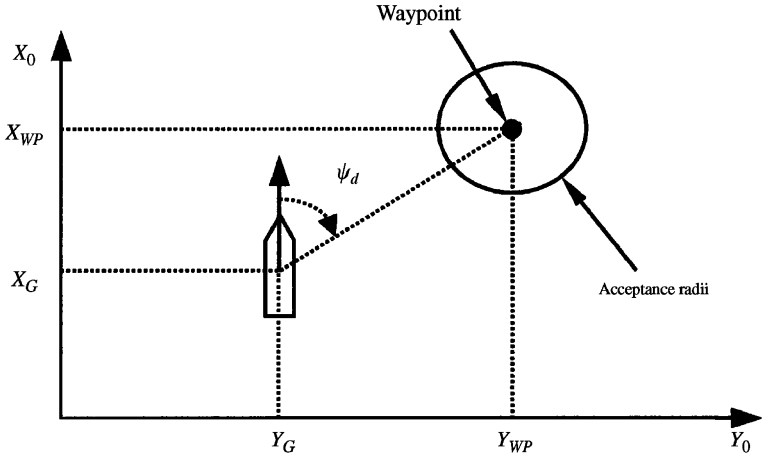

Fig. 1. Line-of-sight (LOS) guidance.

and can be derived as below

$$\begin{bmatrix} \dot{v} \\ \dot{r} \\ \dot{\psi} \end{bmatrix} = \begin{bmatrix} a_{11} & a_{12} & 0 \\ a_{21} & a_{22} & 0 \\ 0 & 1 & 0 \end{bmatrix} \begin{bmatrix} v \\ r \\ \psi \end{bmatrix} + \begin{bmatrix} b_1 \\ b_2 \\ 0 \end{bmatrix} \delta_\psi \tag{19}$$

or simply expressed as

$$\dot{\boldsymbol{x}}_{\boldsymbol{h}} = \boldsymbol{A}_{\boldsymbol{h}}\boldsymbol{x}_{\boldsymbol{h}} + \boldsymbol{b}_{\boldsymbol{h}}\boldsymbol{\delta}_{\boldsymbol{\psi}}. \tag{20}$$

The sliding surface expresses the control error composed of sway velocity error, yaw rate error and heading angle error. It is practical to set the desired sway velocity and desired yaw rate as zero to make the ship sailing on the desired course. Therefore, the sliding surface σ_h is defined as

$$\sigma_h = h_1 v + h_2 r + h_3(\psi - \psi_d) \tag{21}$$

where $h_i (i = 1, 2, 3)$ are the components of right eigenvector $\boldsymbol{h}$. In order to stabilize the sway–yaw dynamics, the feedback gain vector can be set as $\boldsymbol{k} = [k_1, k_2, 0]^{\mathrm{T}}$ such that:

$$A_C = A_h - b_h k^T = \begin{bmatrix} a_{11} - b_1 k_1 & a_{12} - b_1 k_2 & 0 \\ a_{21} - b_2 k_1 & a_{22} - b_2 k_2 & 0 \\ 0 & 1 & 0 \end{bmatrix}. \tag{22}$$

Here, $k_3 = 0$ means the linear feedback from yaw angle is not necessary to stabilize the sway-yaw dynamics. The characteristic equation corresponding to the upper left 2×2 submatrix of $\boldsymbol{A}_C$ is written as

$$(a_{11} - b_1 k_1 - \lambda)(a_{22} - b_2 k_2 - \lambda) - (a_{21} - b_2 k_1) \times (a_{12} - b_1 k_2) = 0. \tag{23}$$

From Eq. (23), k_1 and k_2 can be solved by any value of λ (i.e. λ_1 and λ_2). Consequently $\boldsymbol{A}_C$ are decided and the right eigenvector $\boldsymbol{h}$ can be obtained from $A_C^{\mathrm{T}} h = 0$ corresponding to $\lambda_3 = 0$. Then the sliding mode control law for δ_ψ becomes

$$\delta_\psi = -(k_1 v + k_2 r) + (h_1 b_1 + h_2 b_2)^{-1}\left[-\eta_h \tanh\left(\sigma_h/\phi_h\right)\right], \tag{24}$$

where η_h is heading switching gain and ϕ_h is the boundary layer thickness.

Concerning the roll response and neglecting the other motion coupling effect, Eq. (4) is simplified as a linear one,

$$(I_{xx} + J_{xx})\dot{p} = -K_{\dot{\phi}} p + K_\delta \delta_\phi, \tag{25}$$

where p is roll rate $\left(p = \dot{\phi}\right)$, $K_{\dot{\phi}}$ is roll damping coefficient and K_δ is the rudder coefficients of linearized rudder moment. Eq. (25) can be regarded as the first-order equation of p, then the sliding surface for roll response control can be easily defined as $\sigma_{\mathrm{R}} = p - p_{\mathrm{d}}$. Since the desired roll angle is zero, the desired roll rate p_{d} is also zero. Therefore, the sliding mode control command for roll reduction δ_ϕ is obtained by

$$\delta_\phi = K_\delta^{-1}\left[K_{\dot{\phi}} p - (I_{xx} + J_{xx})\eta_{\mathrm{R}} \tanh\left(\sigma_{\mathrm{R}}/\phi_{\mathrm{R}}\right)\right], \tag{26}$$

where η_{R} is roll switching gain and ϕ_{R} is the boundary layer thickness.

3.2. Compact control

In the above, the separate control system composes of two subsystems for sway–yaw and roll. However, the sway, roll, and yaw interactions may play an important role on control ability. Therefore the so-called "Compact Control" for sway–roll–yaw is linearized from Eqs. (2), (4), and (6) and can be derived as below

$$\begin{bmatrix} \dot{v} \\ \dot{r} \\ \dot{p} \\ \dot{\psi} \end{bmatrix} = \begin{bmatrix} a_{11} & a_{12} & a_{13} & 0 \\ a_{21} & a_{22} & a_{23} & 0 \\ a_{31} & a_{32} & a_{33} & 0 \\ 0 & 1 & 0 & 0 \end{bmatrix} \begin{bmatrix} v \\ r \\ p \\ \psi \end{bmatrix} + \begin{bmatrix} b_1 \\ b_2 \\ b_3 \\ 0 \end{bmatrix} \delta. \tag{27}$$

The roll angle is not included because a stable disturbance will cause a steady roll response. The sliding surface is defined as $\sigma_c = h_1 v + h_2 r + h_3 p + h_4(\psi - \psi_{\mathrm{d}})$. Using the same derivation process as stated above, the

compact sliding mode controller can be obtained by

$$\delta = -(k_1 v + k_2 r + k_3 p) + (h_1 b_1 + h_2 b_2 + h_3 b_3)^{-1} \times \left[-\eta_c \tanh(\sigma_c/\phi_c)\right], \quad (28)$$

where η_c is heading switching gain and ϕ_c is the boundary layer thickness.

4. Genetic algorithm

In order to make the control optimal, the separate control with four design parameters (λ_1, λ_2, η_h, ϕ_h) in Eq. (24) and two parameters (η_R, ϕ_R) in Eq. (26) must be well tuned. Similarly the compact control described in Eq. (28) has five design parameters need tuning, i.e. three eigenvalues, η_c and ϕ_c. This task is generally time-consuming and difficult to handle, therefore the genetic algorithm (McGookin et al., 2000) is adopted to reach this purpose. The genetic algorithm is a powerful parameter optimization technique and the string of integers is adopted here to search optimum. An integer string (called chromosome) contains a set of parameters and each individual integer value (i.e. from 0 to 9 in this study) represents a gene. Here, each design parameter is composed of five genes (e.g. A, B, C, D, and E) and the decoding formula is defined as

$$\text{Parameter} = [A \times 1 + B \times 0.1 + C \times 0.01 + D \times 0.001] \times 10^{(E/2-2)}. \quad (29)$$

In Eq. (29), the exponent of 10 is adjusted to an integer value between -2 and 3. Therefore, this process could provide real values between 0.001×10^{-2} and 9.999×10^{3} to obtain optimal parameters. Since there are at most six parameters needed to be tuned, the number of genes in each chromosome is 30.

The general procedure for the genetic algorithm is shown in Fig. 2. After defining gene and chromosome, the first step is building an initial population of chromosome randomly. When the initial population is accomplished, the cost value can be got from ship motion simulation in time domain. Through the ascending sort of cost values, the operation of reproduction is made according to rank-based selection which better chromosomes with lower cost values (i.e. 20% in this study) are kept for the next population and others are formed through crossover and mutation of the current population. This type using elite reproduction scheme is called an Elite Genetic Algorithm, and this elite reproduction scheme will provide better solution than classical reproduction scheme (Brooks et al., 1996). Two-point crossover is used in crossover operation, parent chromosomes for crossover operation are randomly chosen from the current population and no weighting based on the quality of the chromosome is performed. This process is repeated until the new built chromosomes are enough to replace the 80% of the current population with poorer cost values. Mutation is the random selection of new population's genes and the random change of the selected genes values (i.e. the genes values are randomly changed between 0 and 9). The held elite chromosomes are unaffected in this process. After one process of cost evaluation, sort, reproduction, crossover and mutation, a new population is formed as the next generation. Repeating the same process, the approximately optimal generation will be obtained through the genetic algorithm. In this study, the population size (chromosome numbers) is 50, mutation rate is 5% of new population's genes, and the generation size is 100.

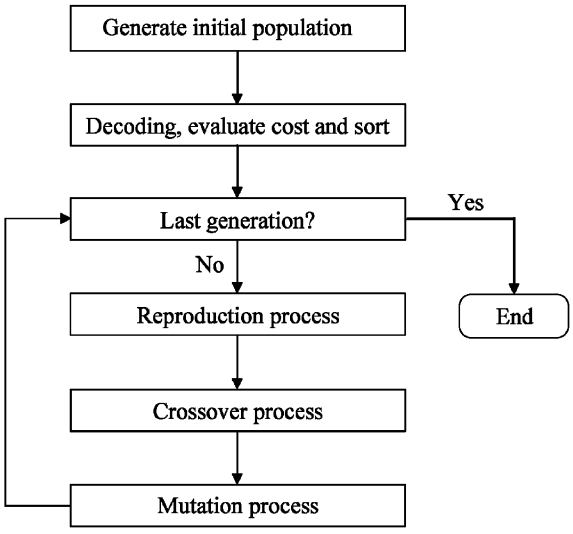

Fig. 2. Genetic algorithm flow chart.

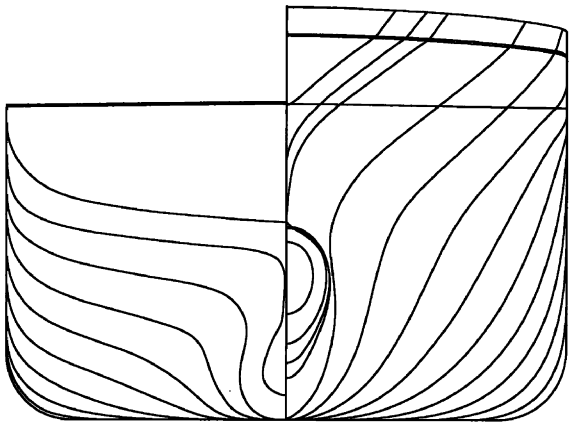

Fig. 3. Body plan of container ship.

The following cost function is used for the judgment while doing the optimization process by genetic algorithm:

$$C_{\text{TOTAL}} = \sum_{i=0}^{S} \left[\alpha_1 (\Delta\psi_i)^2 + \alpha_2 \delta_i^2 + \phi_i^2\right]. \quad (30)$$

The right-hand side of Eq. (30) is related to the track keeping and roll motion, in which S is the total number of iterations in the time simulation process, $\Delta\psi_i$ is the ith heading error between desired heading and actual heading, δ_i is the ith rudder angle, ϕ_i is the ith roll angle, α_1 and α_2 are weighting factors.

In order to investigate the efficiency of the present sliding mode controller on the roll reduction for the ship maneuvering in random sea, the percentage of roll reduction (Jerrold and Michael, 1999) is defined as

$$\text{Roll reduction (\%)} = \frac{\text{AP} - \text{RRC}}{\text{AP}} \times 100, \tag{31}$$

where AP is the standard deviation of roll angle calculated from the autopilot controller without roll reduction, i.e. $\delta = \delta_\psi$ in Eq. (18), while RRC is the one including roll reduction control.

Table 1
The principal particulars of ships

Length (perpendicular) (m)	185.5
Breadth (m)	30.2
Depth (m)	16.6
Draft (m)	11
Trim (aft) (m)	0
Metacentric height (m)	2
Displacement volume (m^3)	41700
Block coefficient	0.6651
Prismatic coefficient	0.6775
Waterline coefficient	0.8561

5. Results and discussion

In this paper, the simulation of ship maneuvering with autopilot control system in random waves is investigated. A straight line is set as the course to guide the ship sailing to the forward direction with different sea states. A container ship is selected to simulate the motion responses, the body plan is shown in Fig. 3, and the principal particular is listed in Table 1. The initial ship speed of container ship is 23 knots. The maximum rudder deflection and the rate limit are set to be 35° and 3.5°/s, respectively. For simplification, the water depth is assumed to be infinitely deep.

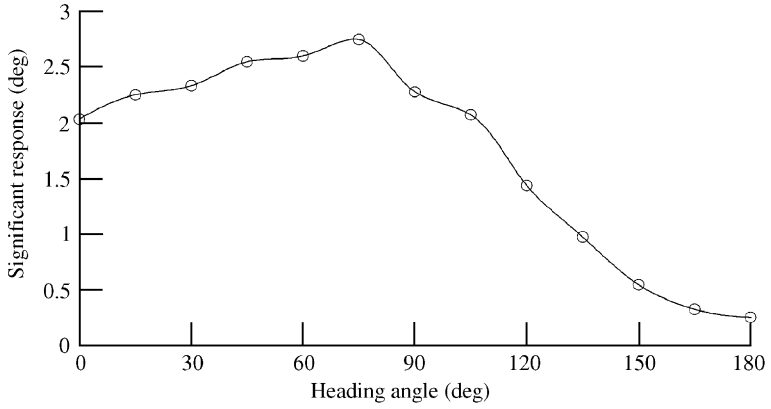

Fig. 4. The significant roll response at random wave (ship speed 23 knots, $H_{1/3} = 3\,\text{m}$ and $\bar{T} = 10\,\text{s}$).

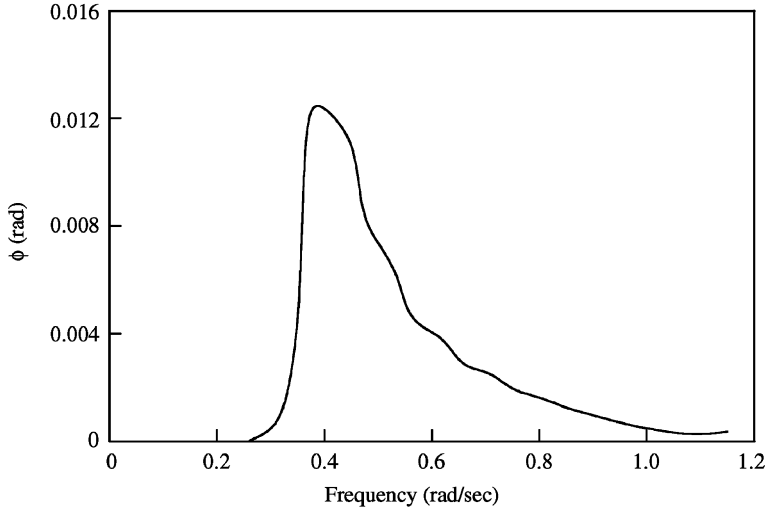

Fig. 5. The RAO analysis of roll response at corresponding heading and ship speed (heading 75°, ship speed 23 knots, $H_{1/3} = 3\,\text{m}$, and $\bar{T} = 10\,\text{s}$).

In the present study, three kinds of sliding mode controls on the rudder are investigated, i.e. for track keeping control only, and track keeping including roll reduction by separate control or compact control. Therefore, three sets of design parameters must be decided first. The track keeping control needs only four parameters (λ_1, λ_2, η_h, ϕ_h) whereas the separate control needs six parameters (λ_1, λ_2, η_h, ϕ_h, η_R, ϕ_R) to execute the track keeping and roll reduction functions, and five parameters (λ_1, λ_2, λ_3, η_c, ϕ_c) are needed for the compact control. Because determining optimal design parameters takes huge time, it is not recommended to apply genetic algorithm directly in random wave simulation. The alternative way is adopting the regular wave simulation with peak wave frequency decided by the response amplitude operation (RAO). Fig. 4 is the significant roll response for the container model in random wave with $H_{1/3} = 3$ m and $\bar{T} = 10$ s, and the peak value appears at heading angle 75°. Under this condition, we can find the peak wave frequency is 0.39 rad/s from the related spectrum as shown in Fig. 5. According to the above conditions and assumed regular wave height 3 m, the genetic algorithm is employed to obtain the approximate optimal design parameters for the control simulation. The corresponding design parameters are listed in Table 2.

The time domain simulation for ship motions in random waves is done by fourth-order Runge–Kutta numerical integration method with the time interval of 0.1 s. The waypoints (X_{WP}, Y_{WP}) for guidance is set as (1339.75, 5000). Based on the wave with $H_{1/3} = 3$ m and $\bar{T} = 10$ s, the simulation results of roll responses, heading error and rudder deflection are presented in Fig. 6. The dash line presents the simulation results using track keeping control

Table 2
Design parameters

	λ_1	λ_2	η_h	ϕ_h	η_R	ϕ_R
Track keeping control	−2.681	−0.084	0.1005	4.057		
Separate control	−0.0125	−0.1121	8.692	3.48	969.6	71.8
	λ_1	λ_2	λ_3	η_c	ϕ_c	
Compact control	−3.897	−0.026	−0.01271	0.0285	4.802	

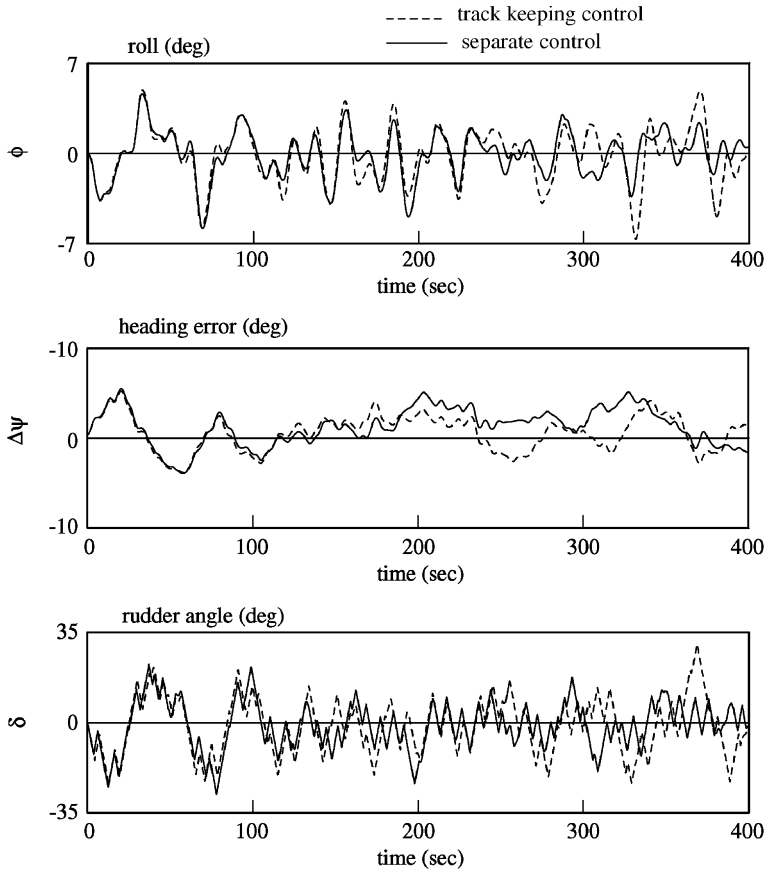

Fig. 6. The simulation result comparison between track keeping control and separate control.

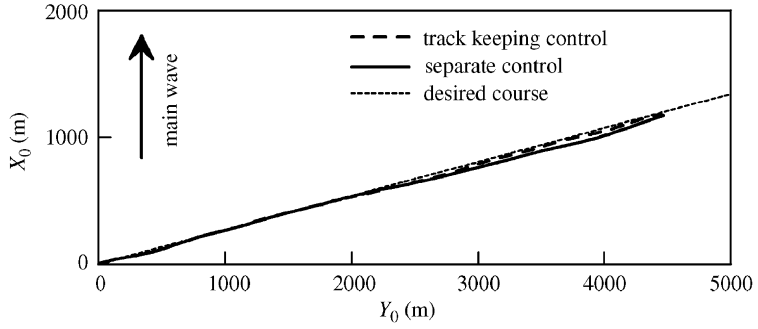

Fig. 7. The simulation trajectories of track keeping control and separate control at initial heading 75° $H_{1/3} = 3$ m, and $\bar{T} = 10$ s).

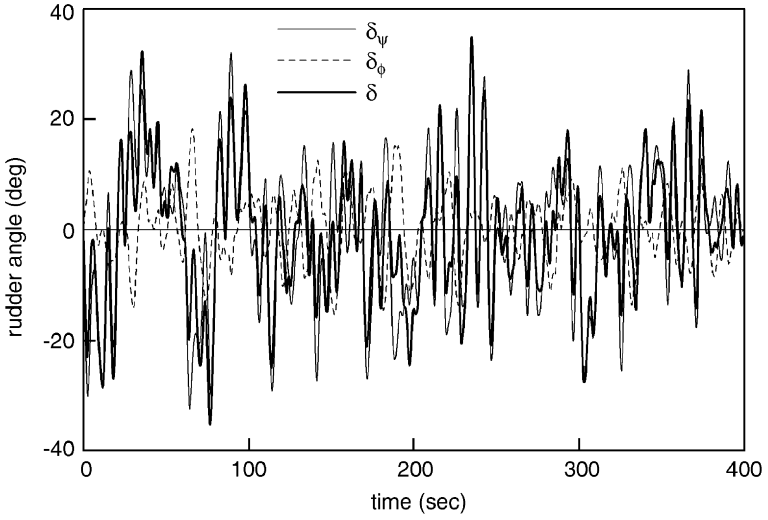

Fig. 8. The rudder command of separate control before rudder deflection limitation.

without roll reduction control (i.e. $\delta = \delta_\psi$) while the solid line is the separate control with the roll reduction control (i.e. $\delta = \delta_\psi + \delta_\phi$). From this figure, the roll response is indeed improved when the roll reduction control is included, but heading error increases. At this sea state, roll reduction percentage 15.48% is obtained (i.e. Eq. (31)) which proves the roll reduction control indeed works. The trajectory shown in Fig. 7 presents both control types are well done to navigate the container ship sailing to the desired course, and the trajectory using track keeping control without roll reduction consideration is closer to the course than the separate controller with roll reduction control. Fig. 8 is the component of rudder command calculated from separate control whose amplitude varied with track keeping and roll reduction command. Before the rudder actuator acts, this separate rudder command is judged by the maximum rudder angle and rate limit to achieve a reasonable rudder operating.

Fig. 9 is the simulation result comparison between track keeping control and compact control. The result reveals that 17.69% roll reduction is obtained by using the compact control which seems better than the separate one. The cost values calculated from the cost function are listed in Table 3, which indicates both the separate control and compact control reduce the roll response with more heading error and less rudder action. These values show that the compact control has better roll reduction function, but has larger heading error and rudder deflection than the separate control. Fig. 10 is the trajectories comparison between track keeping control and compact control, the trajectory presents the compact control behaves well to navigate the container ship. Similar to the result shown in Fig. 7, the trajectory obtained by track keeping control is better than that by compact control because the latter needs to handle the roll reduction.

6. Conclusion

In this paper, ship autopilot system is adopted to investigate the ability of track keeping and roll reduction in random waves by rudder control. Both the separate sliding mode controller and compact sliding mode controller are successful to accomplish the autopilot mission with track keeping and roll reduction. The design parameters for both controllers have been optimized by genetic algorithm instead of artificial adjustment. In order to save

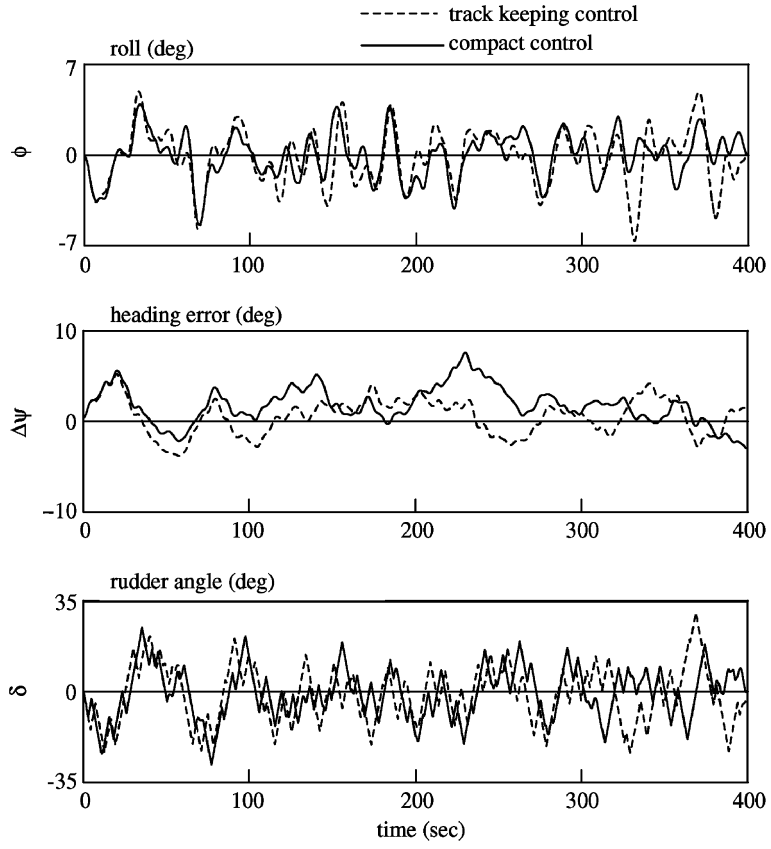

Fig. 9. The simulation result comparison between track keeping control and compact control.

Table 3
Cost values of simulation results

	Heading error	Rudder usage	Roll response
Track keeping control	5040.183	17751.67	36994.65
Separate control	7201.132	12952.55	26383.54
Compact control	8934.854	14293.45	24937.95

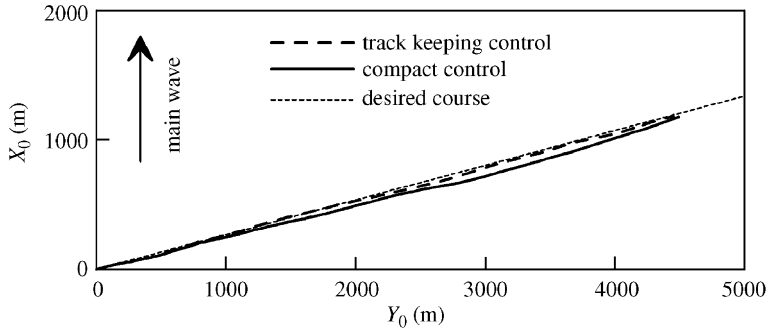

Fig. 10. The simulation trajectories of track keeping control and compact control at initial heading 75° ($H_{1/3} = 3$ m, and $\bar{T} = 10$ s).

time-consuming for the calculation during the optimization process, the optimal design parameters are decided according to the heading angle with the largest RAO of roll motion in regular wave.

The separate controller needs six design parameters, i.e. four are for track keeping control, and two are for the roll reduction, whereas the compact controller needs five ones. The present simulation results show that the track keeping

and roll reduction can be both achieved generally and the compact controller gets better roll reduction. Although the compact control can get more roll reduction and only five design parameters are needed to be decided, there exist more rudder action which is not good for the rudder and its derivative process is more complicated because of coupling terms. Therefore, it is suggested to use the separate control if the roll reduction is considered.

The simplified and practical hydrodynamic model with maneuvering and seakeeping characteristics presented here is successful to simulate the ship motion responses in random waves. It is useful for naval architects to analyze the corresponding behavior of a ship maneuvering in waves with the functions of autopilot and roll reduction.

References

Bailey, P.A., 1999. Maneuvering of a ship in a seaway. Ph.D. Thesis. University of Southampton, UK.

Baitis, A.E., Schmidt, L.V., 1989. Ship roll stabilization in the U.S. navy. Naval Engineers Journal 101 (3), 43–53.

Brooks, R.R., Iyengar, S.S., Chen, J., 1996. Automatic correlation and calibration of noisy sensor readings using elite genetic algorithms. Artificial Intelligence 84, 339–354.

Crossland, P., Johnson, M.C., 1998. A time domain simulation of deck wetness in head seas. In: Proceedings RINA International Conference on Ship Motions and Manoeuverability, London, UK.

Dove, M.J., Wright, C.B., 1991. Development of marine autopilots. In: Computer Methods in Marine and Offshore Engineering. Computational Mechanics Publication, Southampton, pp. 259–272.

Fang, M.C., 1991. Roll reduction by rudder control for two ships during underway replenishment. Journal of Ship Research 35, 141–150.

Fang, M.C., Lee, M.L., Lee, C.K., 1993. The simulation of water shipping for a ship advancing in large longitudinal waves. Journal of Ship Research 37, 126–137.

Fossen, T.I., 1994. Guidance and Control of Ocean Vehicles. Wiley, New York.

Funaji, S., Kijima, K., Furukawa, Y., 2003. Ship maneuvering performance under the influence of external disturbances. Transaction of the West–Japan Society of Naval Architects 106, 47–56 (in Japanese).

Hamamoto, M., Kim, Y.S., 1993. A new coordinate system and the equations describing maneuvering motion of a ship in waves. Journal of the Society of Naval Architects of Japan 173, 209–220 (in Japanese).

Hamamoto, M., Matsuda, A., Ise, Y., 1994. Ship motion and the dangerous zone of a ship in severe following seas. Journal of the Society of Naval Architects of Japan 175, 69–78 (in Japanese).

Healey, A.J., Lienard, D., 1993. Multivariable sliding mode control for autonomous diving and steering of unmanned underwater vehicles. IEEE Journal of Oceanic Engineering 18 (3), 327–339.

Hirano, M., 1980. On the calculation method of ship maneuvering motion at initial design phase. Journal of the Society of Naval Architects of Japan 147, 144–153 (in Japanese).

Inoue, S., Hirano, M., Kijima, K., Takashina, J., 1981. A practical calculation method of ship maneuvering motion. International Shipbuilding Progress 28, 207–222.

Jerrold, N.S., Michael, G.P., 1999. Rudder/fin roll stabilization of the USCG WMEC 901 class vessel. Marine Technology 36 (3), 157–170.

Mcgookin, E.W., Murray-smith, D.J., Li, Y., Fossen, T.I., 2000. Ship steering control system optimization using genetic algorithms. Control Engineering Practice 8 (4), 429–443.

Munif, A., Umeda, N., 2000. Modeling extreme roll motions and capsizing of a moderate-speed ship in astern waves. Journal of the Society of Naval Architects of Japan 187, 51–58.

Treakle, T.W., Mook, D.T., Liapis, S.I., Nayfeh, A.H., 2000. A time-domain method to evaluate the use of moving weight to reduce the roll motion of a ship. Ocean Engineering 27 (12), 1321–1343.

Umeda, N., Hashimoto, H., 2002. Qualitative aspects of nonlinear ship motions in following and quartering seas with high forward velocity. Journal of Marine Science and Technology 6, 111–121.